



**Environmental  
Science**  
Nano

**Transport of Food- and Catalytic-Grade Titanium Dioxide  
Nanoparticles in Controlled Field Streams with Varying  
Streambed and Biofilm Conditions**

Journal:	<i>Environmental Science: Nano</i>
Manuscript ID	EN-ART-09-2019-001007
Article Type:	Paper

**SCHOLARONE™**  
Manuscripts

### Environmental Significance

Titanium dioxide nanoparticles (NPs) are commonly used in consumer, food, and pharmaceutical products and they are likely to enter the environment upon disposal. Identifying how NPs transport in stream networks is critical to understanding their impact on stream ecology. Lab-scale studies cannot accurately describe the complexity of real streams and there is a need for datasets from larger, more realistic scales. This study uses controlled, field-scale streams to evaluate the transport behavior of catalytic- and food-grade NPs as a function of streambed substrate size and biofilm conditions. Outcomes highlight the importance of considering stream-subsurface exchange and the presence of biofilms, which enhance retention in the streams.

1  
2  
3 **Transport of Food- and Catalytic-Grade Titanium Dioxide Nanoparticles in Controlled**  
4  
5 **Field Streams with Varying Streambed and Biofilm Conditions**  
6  
7  
8  
9

10 **Authors:**

11  
12 Junyeol Kim<sup>a</sup>, Kevin R. Roche<sup>a</sup>, John Sticha<sup>a</sup>, Ariel J. Shogren<sup>b</sup>, Diogo Bolster<sup>a</sup>, Kyle Doudrick<sup>a\*</sup>  
13  
14  
15  
16

17 **Affiliations:**

18  
19 <sup>a</sup>Department of Civil and Environmental Engineering and Earth Sciences, University of Notre  
20  
21 Dame, Notre Dame, IN 46556  
22  
23

24 <sup>b</sup>Department of Earth and Environmental Sciences, Michigan State University, East Lansing, MI  
25  
26 48824  
27  
28  
29

30  
31 **\*Corresponding Authors and Address:**

32  
33 Kyle Doudrick, Department of Civil and Environmental Engineering and Earth Sciences,  
34  
35 University of Notre Dame, Notre Dame, Indiana, USA, 46637  
36

37 Phone: 5746310305

38  
39  
40 e-mail: [kdoudrick@nd.edu](mailto:kdoudrick@nd.edu)  
41  
42  
43

44 JOURNAL: Environmental Science: Nano  
45  
46  
47  
48

49 Revision Date: September 2, 2019  
50  
51  
52  
53  
54  
55  
56  
57  
58  
59  
60

## Abstract

With the increased use of nanoparticles (NPs) in consumer, food, and pharmaceutical products, their eventual release into streams is inevitable. Critical factors affecting the transport of NPs in streams are the hyporheic exchange between the water column and porous streambed substrate and the interaction with biofilms. In this study, the transport behavior of two titanium dioxide NPs – catalytic- (P90) and food-grade (E171) – was evaluated in four field streams lined with different streambed substrate sizes for varying seasonal biofilm conditions. When biofilm growth was minimal, NP retention in the streams increased with increasing substrate size due to increased hyporheic exchange and subsequent physical and chemical interactions between the NPs and substrate. For all streams, the average mass recovery at the 40 m sampling point for E171 and P90 was  $44 \pm 8.7\%$  and  $16 \pm 8.0\%$ , respectively. The greater mobility of E171 was due to the inherent presence of negatively charged surface phosphates that reduced aggregation and decreased its interaction with the substrate. When biofilms were thriving in the streams the average mass recovery at 40 m for both NPs decreased significantly (E171 =  $5.8 \pm 7.3\%$ ,  $P = 0.0017$ ; P90 =  $2.4 \pm 0.7\%$ ,  $P = 0.041$ ), and the mass recovery difference between the two NPs became insignificant ( $P = 0.38$ ).

**Keywords:** Nanoparticle; nanomaterial; titanium dioxide; fate and transport; stream; field

## 1. INTRODUCTION

Engineered nanoparticles (NPs) are an emerging class of materials that are commonly found in consumer, food, and pharmaceutical products.<sup>1-4</sup> Upon their release from products, NPs can enter streams directly or indirectly from wastewater treatment plant and landfill discharges.<sup>5</sup> While there have been numerous controlled lab-scale studies on the environmental transport of NPs (e.g., porous media column tests),<sup>7-27</sup> experimental data is limited for realistic streams where transport will be controlled by surface flows, subsurface interactions, and contact with biofilms. This lack of data inhibits our ability to mathematically predict NP transport at scale of environmental interest.

Hyporheic exchange involves the advective and dispersive transfer of water between the stream and the underlying and adjacent subsurface that is composed of complex porous substrate. Suspended (e.g., NPs) or dissolved materials can be carried with the water into the substrate, where physical, chemical, and biological processes can strongly impact their transport.<sup>28, 29</sup> Aggregation reactions between NPs (i.e., homoaggregation) and between NPs and collectors such as clays (i.e., heteroaggregation) can result in increased settling rates that lead to enhanced hyporheic exchange and shorter transport lengths.<sup>30-46</sup>

Biofilms are a complex assemblage of algae, bacteria, and fungi embedded in extracellular polymeric substances. They are present in streams and can colonize on the surface of the porous substrate or vegetation or they can be suspended in the water column.<sup>47</sup> Biofilms also expected to be a dominant factor controlling downstream transport by immobilizing NPs.<sup>18, 48-53</sup> The presence of biofilms has been shown to increase the retention of NPs in the porous substrate<sup>18, 49, 50, 52, 53</sup> and the water column.<sup>54</sup> In turn, the accumulation of NPs in biofilms can induce negative effects that impact the stream ecology.<sup>55-59</sup>

Predicting transport of anything in streams is complex due to the multivariate, interconnected processes, and these cannot be accurately described using simplistic lab-scale datasets. Thus, there is a need for controlled field studies that can capture realistic behavior. The objective of this study was to evaluate the transport of NPs in controlled field streams as a function of streambed substrate size and seasonal biofilm growth. All stream experiments were conducted at the University of Notre Dame Linked Experimental Ecosystem Facility (ND-LEEF). The ND-LEEF site has four identical experimental streams, which differ only in the size of the streambed substrate lining the bottom. Titanium dioxide ( $\text{TiO}_2$ ) was used as an important and representative NP.  $\text{TiO}_2$  NPs are commonly used as a white pigment in food and personal care products, designated as food-grade  $\text{TiO}_2$  or E171.<sup>60</sup> Most studies investigating the environmental and health implications of  $\text{TiO}_2$  NPs have used catalytic-grade  $\text{TiO}_2$  (e.g., P25 or P90 from Evonik),<sup>61</sup> but using this as a reference material in place of E171 is not suitable<sup>62, 63</sup> due to the differences in size distribution and surface chemistry. The surface of E171 is more negatively charged due to the presence of surface phosphates and stark behavioral differences have been observed compared to catalytic-grade  $\text{TiO}_2$ .<sup>63-67</sup> In this study, we compared the transport behavior of both E171 and P90, and link their aggregation behavior to observed transport outcomes.

## 2. METHODOLOGY

### 2.1 Nanoparticles and Tracers

Two  $\text{TiO}_2$  NPs (P90 and E171) were used for the stream transport experiments. P90 was donated by Evonik (Essen, Germany) and used as received. It is a mixture of anatase (86%) and rutile (14%) with an average primary particle size of 12 nm and 18 nm, respectively.<sup>68</sup> E171 was

1  
2  
3 purchased from Minerals-Water Ltd. (Purfleet, UK) and used as received. E171 is mostly anatase  
4 with a particle size range of  $106\text{--}132 \pm 38\text{--}56$  nm, depending on the manufacturer.<sup>69</sup> The pH  
5 zero point of charge ( $\text{pH}_{\text{zpc}}$ ) of P90 and E171 in an aqueous solution is approximately 6.0 and  
6 4.5, respectively.<sup>70</sup> The lower  $\text{pH}_{\text{zpc}}$  of E171 is attributed to the negatively charged phosphate  
7 groups attached to its surface.<sup>65</sup>  
8  
9

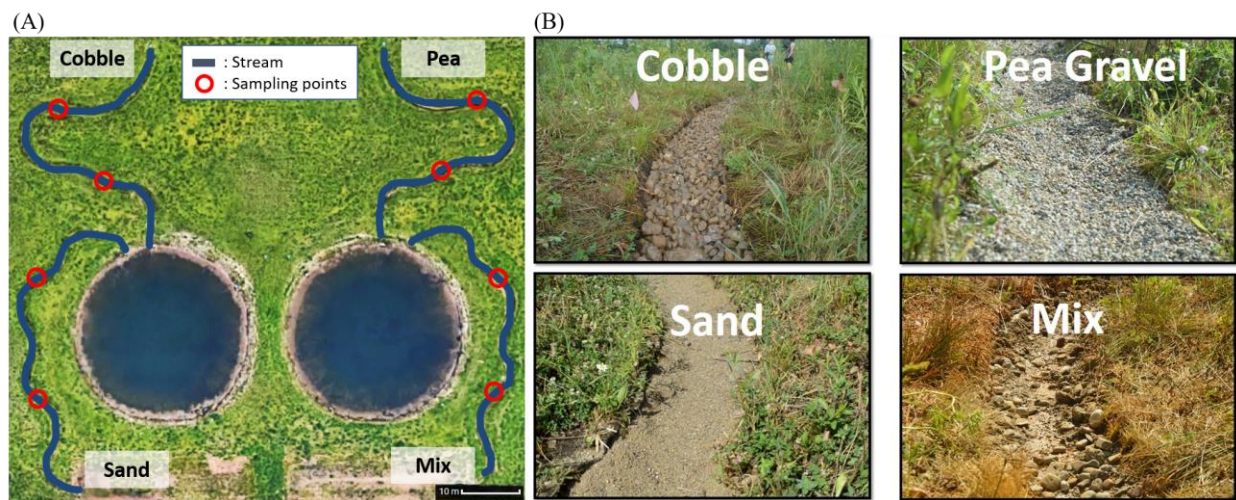
10  
11  
12  
13  
14  
15 Potassium bromide (KBr; Fisher Scientific, Hampton, NH, USA) and rhodamine water  
16 tracer (RWT,  $\text{C}_{29}\text{H}_{29}\text{ClN}_2\text{Na}_2\text{O}_5$ ; Acros Organics, NJ, USA) were used as conservative tracers in  
17 the stream transport experiments. RWT has previously been shown to be suitable for experiments  
18 at ND-LEEF,<sup>71-73</sup> and both RWT and KBr were used in this study interchangeably, depending on  
19 the season and equipment available. KBr was used as a conservative tracer in June when few  
20 biofilms were present. In September, when biofilms were flourishing, RWT was used to  
21 accurately resolve adsorption to biofilms and to obtain a wider range of concentrations.  
22  
23  
24  
25  
26  
27  
28  
29  
30

## 31 32 33 **2.2 ND-LEEF Site Description**

34  
35 Field experiments were conducted in the experimental streams at ND-LEEF, which is located at  
36 St. Patrick's County Park in South Bend, IN, USA (Figure 1A). ND-LEEF is a globally unique  
37 research facility that houses two man-made experimental watersheds, each consisting of an  
38 interconnected pond, two stream reaches, and a wetland. The four experimental streams are  
39 identical in terms of hydraulic gradient, width, and other primary hydraulic characteristics  
40 (Figure S1). Specifically, each stream is 0.4 m wide and 55 m long with a hydraulic gradient of  
41 0.0075. The stream channel base is lined with cement concrete to prevent uncontrolled  
42 hydrologic interactions with the surroundings. Previous studies in these streams have shown that  
43 dilution is minimal as there is no lateral inflow of water.<sup>74</sup> Each streambed has a unique substrate  
44  
45  
46  
47  
48  
49  
50  
51  
52  
53  
54  
55  
56  
57  
58  
59  
60

1  
2  
3 approximately 10 cm thick. In this study, the streams were lined with sand (Sand), pea gravel  
4 (Pea), cobble gravel (Cobble), and a 1:1:1 volume ratio mixture of all three (Mix) (Figure 1B).  
5  
6 The average  $D_{50}$  size of the substrates is 0.053 cm, 0.67 cm, and 5 cm for Sand, Pea, and Cobble,  
7  
8 respectively. Further images and descriptions of the streams can be found elsewhere.<sup>71-73, 75</sup>  
9  
10

11  
12 The streams receive water from a constant-head reservoir supplied by groundwater; the  
13  
14 average hydraulic residence time in the reservoir is approximately 3.5 d before reaching the head  
15  
16 of the streams. The stream baseflow for this study was  $0.8 \text{ L s}^{-1}$ . Prior to turning on the water for  
17  
18 the experimental season, the streams were biologically “reset” by removing terrestrial organic  
19  
20 matter (e.g., leaves) and benthic algae by hand. The top layer of the streambed substrate (~2-5  
21  
22 cm) was physically mixed to mobilize any remaining organic matter. The substrate was then  
23  
24 returned to mostly flat topography aside from natural roughness features created by the substrate.  
25  
26 After water flow was initiated, the streams were allowed to flow for at least 2 days prior to  
27  
28 experiments to naturally flush any loose organic matter.  
29  
30  
31  
32



50 Figure 1. (A) Aerial photograph of ND-LEEF site (obtained from Google Earth) with schematic  
51 detailing stream location and sampling points. (B) Photographs of streambed substrates for each  
52  
53 stream.  
54  
55  
56  
57

### 2.3 Characterization of the Aggregation Behavior of Nanoparticles

The aggregation behavior of P90 and E171 was analyzed using dynamic light scattering (DLS) and phase analysis light scattering (PALS) (NanoBrook Omni, Brookhaven Instrument Corporation, Holtsville, NY). DLS was used to measure changes in the hydrodynamic diameter (HD) over approximately 65 min. A solution of  $10 \text{ mg L}^{-1}$   $\text{TiO}_2$  was prepared in either ultrapure water ( $18.2 \text{ M}\Omega\text{-cm}$ ), or unfiltered stream water (pH 8.12), filtered stream water ( $0.22\text{-}\mu\text{m}$  PTFE membrane). Immediately after adding the  $\text{TiO}_2$  to water, the samples were shaken vigorously and 3 mL was added to a plastic cuvette for DLS measurement. All measurements were conducted at a  $90^\circ$  scattering angle at  $25^\circ\text{C}$  with a 10 s equilibration time. The HD was measured in triplicate and the average and standard error of the effective diameters were reported. PALS was used to measure the zeta potential ( $\zeta$ ) of P90 and E171 in the stream water. No background electrolyte was added to the solutions due to the already existing conductivity.  $10 \text{ mg L}^{-1}$  solutions of  $\text{TiO}_2$  were prepared in the filtered stream water and then mixed for 24 hrs. Samples were then diluted to ( $\sim 100 \mu\text{g L}^{-1}$ ) and added to a plastic cuvette for analysis. Thirty measurement cycles were conducted at a  $15^\circ$  scattering angle and at  $25^\circ\text{C}$  in triplicate, and the average and standard errors are reported. The zeta potential was calculated from electrophoretic mobilities using the Smoluchowski model (i.e.,  $\kappa a > 1$ ).

### 2.4 Stream Experiments

The stream-scale experiments were conducted in both June and September (2018). In June, immediately after the biological “reset”, the biofilm growth was minimal and the streams differed only by their streambed substrate. The streams were then allowed to freely colonize with

1  
2  
3 biofilm throughout the remainder of the summer, resulting in a substantial growth of biofilms  
4  
5 throughout each stream reach, as characterized previously.<sup>76</sup> Transport experiments were then  
6  
7 repeated in September, during peak biofilm biomass (Figure 2).  
8  
9

10 Stream transport and retention of NPs was investigated using short-term solute addition  
11  
12 experiments with pulse injections (e.g.<sup>77</sup>). Before each experiment, background samples were  
13  
14 taken every 10 m (i.e., 0, 10, 20, 30, 40, 50 m). The pH, temperature, and conductivity were  
15  
16 measured on-site, and water column samples were taken for further analyses, including total  
17  
18 suspended solids (TSS), total dissolved solids (TDS), dissolved organic carbon (DOC), major ion  
19  
20 concentrations, and background Ti. For TDS and TSS analysis, filters and crucibles were washed  
21  
22 using water, then dried and weighed. 900 mL of stream water was then filtered through a 0.45-  
23  
24  $\mu\text{m}$  nylon membrane followed by an ultrapure water rinse. The filter was dried in an oven at 105  
25  
26  $^{\circ}\text{C}$  for 1 hr, placed in a desiccator for 10 min, and then weighed to measure TSS. The filtrate was  
27  
28 placed in the crucible, dried in an oven overnight, placed in a desiccator for 10 minutes, and then  
29  
30 weighed to measure TDS. DOC samples were filtered through a 0.45- $\mu\text{m}$  nylon membrane,  
31  
32 acidified, and analyzed using TOC-VCSH (Shimadzu, Addison, IL). Anion and cation  
33  
34 concentrations were analyzed using ion chromatography (IC; ICS-5000, ICS 5000+, AS-23, CS-  
35  
36 12A analytical columns, Thermo Scientific).  
37  
38  
39  
40  
41

42 Conservative tracers were used to evaluate the non-reactive transport behavior in the ND-  
43  
44 LEEF streams in June and September, which corresponds to stream conditions with low and  
45  
46 flourishing biofilms, respectively. In June, a solution of KBr (1 L of 500 mg/L) was used and  
47  
48 samples were taken at 40 m downstream of the  $\text{TiO}_2$  release point. In September, RWT (1 L of  
49  
50 11.48 mg/L) was used, and additional samples were taken at 20 m in addition to the 40 m point  
51  
52  
53  
54 downstream to provide more detailed evidence of the transient transport behavior. The 1 L  
55  
56  
57  
58  
59  
60

1  
2  
3 container of the RWT solution was covered with aluminum foil to prevent any degradation by  
4 the sunlight and vigorously shaken before release into streams. All tracer pulse injections were  
5 quickly poured right above the stream water surface.  
6  
7  
8  
9

10 For TiO<sub>2</sub> NP experiments, the P90 or E171 (1 L, 2 g L<sup>-1</sup>) pulse injections were rapidly  
11 released from a well-mixed container at the top of each stream. The NP solutions were prepared  
12 in ultrapure water and stirred for 24 hrs prior to stream injections, and solutions were vigorously  
13 shaken before release. To avoid cross contamination and minimize variations in the stream  
14 condition, the conservative tracers and TiO<sub>2</sub> NPs experiments were conducted every other day  
15 (e.g., conservative tracer released first day, P90 released in third day, E171 released fifth day,  
16 etc.). The volume and surface area of the substrate (i.e., ~3,675 L of substrate in each stream) is  
17 much greater than the amount of TiO<sub>2</sub> used in each experiment, so influence from prior  
18 experiments would be minimal. Stream samples for NPs were collected using 50 mL conical  
19 centrifuge tubes (Polypropylene, Sterile, VWR, Batavia, IL) at 20 and 40 m from the release  
20 point at the top of the stream. All samples were taken in the channel thalweg, at approximately  
21 half the stream depth.  
22  
23  
24  
25  
26  
27  
28  
29  
30  
31  
32  
33  
34  
35  
36  
37  
38  
39  
40  
41  
42  
43  
44  
45  
46  
47  
48  
49  
50  
51  
52  
53  
54  
55  
56  
57  
58  
59  
60

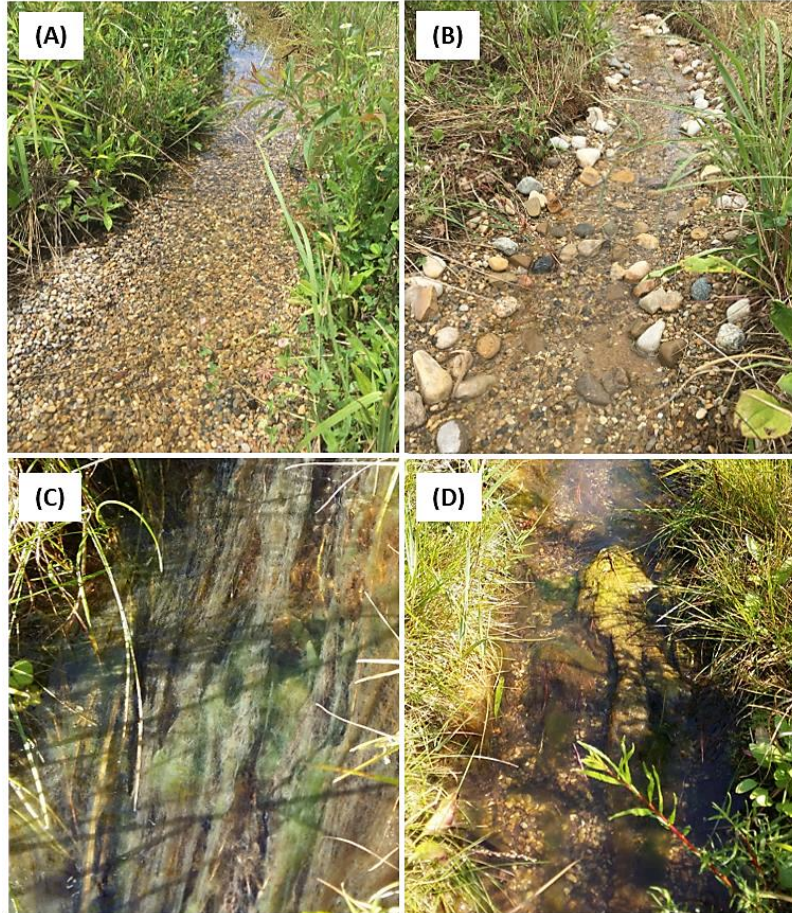


Figure 2. Photographs of streams showing low biofilm and flourishing biofilm growth. (A) Pea stream with low biofilm, (B) mix stream with low biofilm, (C) pea stream with surface biofilms, and (D) pea stream with large biofilm sections. The stream width is 0.4 m.

## 2.5 Quantification of Conservative Tracers and Nanoparticles from Stream Experiments

Samples were transported to the lab and the concentration of bromide was measured using IC. A handheld fluorometer (DataBank™, Turner Designs Inc., San Jose, USA) equipped with a Cyclops submersible sensor (Cyclops-7F, Turner Designs Inc.) was used for *in situ* measurements of the RWT concentration in the streams. Prior to using the fluorometer at ND-LEEF, the sensor was calibrated in the lab under dark conditions. When using the fluorometer,

1  
2  
3 the sensor was placed at the 20 m point of each stream parallel to the streambed. The sensor was  
4 covered completely to prevent any penetration of sunlight that may interfere with the  
5 measurement of RWT. The fluorometer was programmed to measure RWT fluorescence every 2  
6 seconds. At the 40 m point, RWT was sampled manually using 50 mL conical centrifuge tubes  
7 and stored in light-sealed container. The concentration was measured immediately after the  
8 experiment using the handheld fluorometer.  
9

10  
11 The concentration of Ti in the streams was measured using inductively coupled plasma  
12 with optical emission spectroscopy (ICP-OES; Perkin-Elmer Optima 8000). A multi-element  
13 standard solution was (Inorganic Ventures, VA, USA) was used for the quantification of Ti, and  
14 yttrium (Y) was used as an internal standard in the ICP-OES analysis. All sample concentrations  
15 were converted to TiO<sub>2</sub> for reporting. Prior to ICP-OES analysis, samples were treated with  
16 microwave assisted acid digestion (Mars 6, CEM corporation, Matthews, NC) to dissolve TiO<sub>2</sub>  
17 into Ti ions. An Se standard solution (SPEX CertiPrep, NJ, USA) was used as a surrogate to  
18 monitor the efficiency of the TiO<sub>2</sub> acid-digestion. To prepare samples for the digestion, first,  
19 each TiO<sub>2</sub> sample was vigorously shaken for 3 min. Then, 5 mL of TiO<sub>2</sub> sample was pipetted  
20 into a Teflon digestion vessel (PFA, CEM corporation, Matthews, NC), followed by adding 5  
21 mL nitric acid (70%, Trace metal grade, Fisher scientific, Hampton, NH). The microwave  
22 digestion protocol consisted of a 20 min temperature ramp to reach the target temperature 210  
23 °C, which was then held for 45 min. Se (100 µL) was added with a nominal concentration of 100  
24 mg/L to every 20<sup>th</sup> Ti sample for quality assurance of the sample preparation process. After the  
25 digestion, all Ti and Se samples were prepared in ultrapure water with HNO<sub>3</sub> (<5% v/v) and  
26 analyzed with ICP-OES. The method detection limit (MDL) for P90 and E171, as calculated  
27 from eight replicates, was 2.1 and 6.3 µg/L, respectively.  
28  
29  
30  
31  
32  
33  
34  
35  
36  
37  
38  
39  
40  
41  
42  
43  
44  
45  
46  
47  
48  
49  
50  
51  
52  
53  
54  
55  
56  
57  
58  
59  
60

## 2.6 Analysis of Breakthrough Curves

The stream experimental data is plotted as a breakthrough curve (BTC), which describes the change in concentration as a function of time for a single point in the stream (i.e., 40 m). Temporal moment analysis of the BTCs was used to evaluate mass transport behavior, calculated using the following equations for the 0<sup>th</sup> ( $M_0$ ), 1<sup>st</sup> ( $M_1$ ), and 2<sup>nd</sup> ( $M_2$ ) moments:<sup>78-80</sup>

$$M_0 = \int_0^t c(x, t) dt$$

$$M_1 = \int_0^t t c(x, t) dt$$

$$M_2 = \int_0^t t^2 c(x, t) dt$$

Where,  $c(x, t)$  ( $M \cdot T \cdot L^{-3}$ ) is concentration at downstream location  $x$  and time  $t$ ,  $Q$  is volumetric flowrate ( $L^3 \cdot T^{-1}$ ),  $M_0$  is the total area of the BTC, which is used to calculate the total mass recovery of NPs the stream reach (i.e., mass recovery or  $MR = M_0 \cdot Q$ ),  $M_1$  informs about the mean arrival time ( $T^2 \cdot M \cdot L^{-3}$ ),  $M_2$  provides information on the spread of the pulse injection as it advects downstream ( $T^3 \cdot M \cdot L^{-3}$ ). For analysis of the BTCs, we used the normalized 1<sup>st</sup> moment,  $M_1/M_0$ , which indicates the plume's mean arrival time ( $T$ ), and the normalized central 2<sup>nd</sup> moment, which describes the variance (or plume spread) of the BTC, calculated as  $M_2/M_0 - (M_1/M_0)^2$  ( $T^2$ ). The integrals were estimated using the trapezoidal rule.

Statistical analysis was done using a two-tailed paired two-sample mean t-test. Exact  $P$  values are reported, and significance was determined herein using an  $\alpha = 0.05$ .

## 3. RESULTS AND DISCUSSION

### 3.1 Characterization of the Stream and Nanoparticle Background Parameters

Background environmental parameters (i.e., ionic strength, pH, conductivity, TSS, TDS, and DOC) of the streams were analyzed in June and September (Table 1). Except for TSS and TDS, parameters differed by less than 5% between streams. Significant seasonal differences were observed for ionic strength ( $P = 0.023$ ), conductivity ( $P = 1.1 \times 10^{-6}$ ), TDS ( $P = 0.001$ ), and DOC ( $P = 8.3 \times 10^{-5}$ ). TDS and conductivity increased because the concentration of cations (e.g.,  $\text{Mg}^{2+}$  and  $\text{Ca}^{2+}$ ) and anions ( $\text{Cl}^-$  and  $\text{SO}_4^{2-}$ ) increased (Table S1), and the increased DOC is likely a result of seasonal biofilm growth (i.e., Figure 2).

Table 1. Background water quality characterization of ND-LEEF streams for June and September. All values are for a composite sample consisting of samples taken every 10 m in the stream ( $n = 6$ ).

	<b>Month</b>	<b>Sand</b>	<b>Pea</b>	<b>Cobble</b>	<b>Mix</b>
Ionic Strength (M)	Jun	0.017	0.017	0.017	0.017
	Sept	0.018	0.021	0.021	0.021
pH	Jun	8.22	8.12	8.16	8.19
	Sept	8.19	8.10	8.10	8.10
Conductivity ( $\mu\text{s}$ )	Jun	462	464	466	467
	Sept	544	547	547	547
TSS (mg/L)	Jun	1.68	1.11	1.10	0.53
	Sept	1.60	2.61	3.56	0.84
TDS (mg/L)	Jun	326	344	350	331
	Sept	397	407	398	397
DOC (mg/L)	Jun	8.44	9.80	9.83	10.32
	Sept	12.4	10.9	12.2	11.4

Figure 3 shows the change in the average HD for P90 and E171 prepared in ultrapure water, unfiltered stream water, and filtered stream water over approximately 65 min. After 30 s of mixing, the average HD of P90 in ultrapure water, unfiltered stream water, and filtered stream water was approximately  $260 \pm 2.46$  nm,  $1130 \pm 94.8$  nm, and  $1200 \pm 113$  nm, respectively. The average HD of E171 in these respective matrices after 30 s was  $300 \pm 6.85$  nm,  $486 \pm 11.5$  nm, and  $510 \pm 7.44$  nm. The average primary particle size of P90 and E171 is approximately  $16 \text{ nm}^{68}$

1  
2  
3 and  $106\text{--}132 \pm 38\text{--}56$  nm ( $n = 5$  manufacturers<sup>69</sup>), respectively. Thus, the short-term DLS time-  
4  
5 point results indicate that rapid aggregation occurred for both NPs using the primary particle size  
6  
7 as a reference point, with more aggregation observed for P90 than E171. This agrees well with  
8  
9 reported sizes for similar TiO<sub>2</sub> NPs, where HDs reach approximately 200 to 300 nm in ultrapure  
10  
11 water and 1200 to 1800 nm in high ionic strength water containing calcium, magnesium, and  
12  
13 chloride ions.<sup>46, 81, 82</sup>

14  
15  
16  
17 After approximately 65 min of mixing, the average HD of P90 in ultrapure water,  
18  
19 unfiltered stream water, and filtered stream water was approximately  $257 \pm 5.28$  nm,  $1940 \pm 179$   
20  
21 nm,  $2060 \pm 34.2$  nm, respectively. The average HD of E171 in these respective matrices after 65  
22  
23 min was  $384 \pm 107$  nm,  $480 \pm 18.2$  nm, and  $661 \pm 22.1$  nm. For P90 in ultrapure water, the HD  
24  
25 did not increase beyond the first sample, but significant aggregation was observed for unfiltered  
26  
27 ( $P = 0.003$ ) and filtered ( $P = 0.015$ ) stream water, with an HD nearly two-fold greater. For E171,  
28  
29 the increase in HD for all matrices was minimal, with only the filtered sample showing any  
30  
31 significant change ( $P = 0.011$ ). These TiO<sub>2</sub> aggregation results agree with reported literature  
32  
33 values  
34  
35  
36

37  
38 For P90, there was no significant difference between filtered and unfiltered samples ( $P =$   
39  
40  $0.36$ ), indicating its size growth was dominated by homoaggregation and not heteroaggregation,  
41  
42 which agrees with the relatively low TSS concentration in the streams (i.e., Table 1). Though the  
43  
44 HD of E171 was greater in the stream water than ultrapure water, it remained relatively stable  
45  
46 over time compared to P90. This is due to the inherent negatively charged phosphates bound to  
47  
48 the surface of E171<sup>69</sup> [i.e.,  $\zeta$  (P90)  $\approx -20$  mV,  $\zeta$  (E171)  $\approx -40$  mV in stream water; Figure S2],  
49  
50 and this agrees with previous studies showing the increased stability of TiO<sub>2</sub> with adsorbed  
51  
52 phosphates.<sup>83, 84</sup>  
53  
54  
55  
56  
57  
58  
59  
60

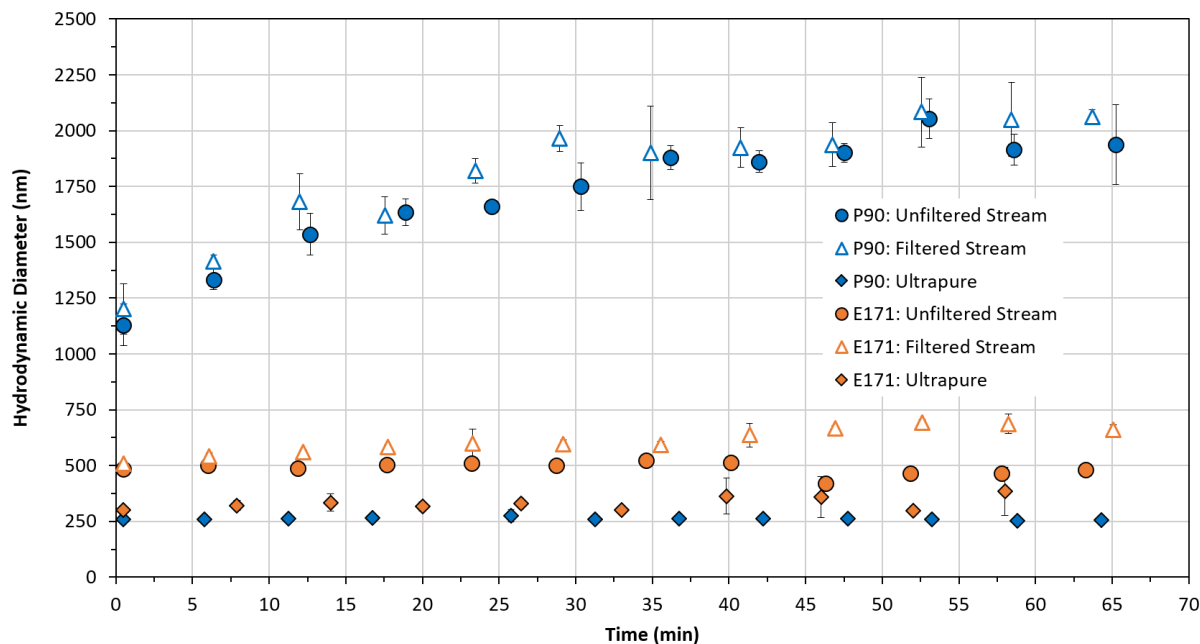


Figure 3. The average hydrodynamic diameter as a function of time for P90 and E171 in unfiltered stream water, filtered stream water, and ultrapure water. The stream water taken from the ND-LEEF site. The error bars represent the standard deviation of three analytical replicates.

### 3.2 Effect of the Streambed Substrate Size on the Transport of P90 and E171

The BTCs for the pulse injections of the conservative tracer, P90, and E171 during low biofilm growth conditions (June) are shown in Figure 4, and results of the moment analysis are provided in Table S2. Figure 5 shows the mass recovery as a function of the mean arrival time for all experiments. For the tracers, the streambed order of mean arrival time and plume spread at 40 m was Sand < Mix ~ Pea < Cobble. For P90 and E171, the mean arrival time order at 40 m was Sand < Pea < Mix < Cobble, and plume spread order was Sand < Mix < Pea < Cobble. The trends were similar for the NPs and the conservative tracer, and there was a proportional relationship between the streambed substrate size and the arrival time and plume spread. This suggests that the transport of all samples was controlled by processes associated with streambed

1  
2  
3 substrate size, including hyporheic exchange and in-stream dispersion due to variability in the  
4  
5 substrate roughness. The mean arrival times increased with increasing substrate size so  
6  
7 hyporheic exchange plays a major role in the transport behavior. Similar behavior has been  
8  
9 observed for transport of kaolinite particles, where a considerably higher percentage of particles  
10  
11 permeated through the pores of coarser sands compared to finer sands,<sup>85</sup> which resulted in a  
12  
13 reduced transport; however, contrasting behavior was observed for environmental DNA in the  
14  
15 ND-LEEF streams.<sup>71</sup> The transport of environmental DNA was reduced in the finer streambed  
16  
17 substrate compared to coarser substrate, which suggests that mechanical straining of the larger  
18  
19 DNA fragments was the dominant retention mechanism. Rather, once exposed to the stream  
20  
21 water, the NPs aggregated (i.e., Figure 3), but transport was still fastest in the sand streams  
22  
23 suggesting other mechanisms were responsible for the observed differences in the mean arrival  
24  
25 time.  
26  
27  
28  
29

30  
31       Though the mean arrival times for the NPs and the conservative tracer were similar for  
32  
33 each stream, their mass recoveries were notably different (Figure 5, Table S2). For the  
34  
35 conservative tracer, the mass recovery at 40 m was approximately 80% for Sand, Pea, and  
36  
37 Cobble and 100% for the Mix stream. Presumably, the conservative tracer did not reach 100%  
38  
39 mass recovery due to analytical detection limitations and experimental error. By comparison, the  
40  
41 average mass recovery of P90 and E171 at 40 m for all streams was approximately  $16\% \pm 8.0\%$   
42  
43 and  $44\% \pm 8.7\%$ , respectively, and there was a significant difference between the NPs ( $P = 1.82$   
44  
45  $\times 10^{-5}$ ). The order of decreasing mass recovery was Sand > Mix > Cobble ~ Pea. Because the  
46  
47 mean arrival times for the NP and tracer were similar, but a reduction in mass recovery was  
48  
49 observed, this suggests the NPs followed a similar flow pathway as the solute but were retained  
50  
51 in the streambed substrate through either physical (e.g., straining) or chemical (e.g., adsorption)  
52  
53  
54  
55  
56  
57  
58  
59  
60

1  
2  
3 mechanisms. Likely, retention was due to a combination of both these mechanisms,<sup>26</sup> which  
4 would be increased by NP aggregation in the stream.<sup>8, 10, 41, 46, 86</sup> Thus, the higher mass recovery  
5 observed for E171 was presumably due to its smaller aggregate size and more negatively charged  
6 surface, which would reduce straining and adsorption retention, respectively. The average  $\zeta$  of  
7 P90 and E171 in the stream water was approximately -20 and -40 mV (Figure S2), respectively.  
8 Typically, substrate such as sand is negatively charged,<sup>46</sup> and the negatively charged phosphate  
9 groups on E171 would reduce adsorption through repulsive forces. Further, the increased  
10 magnitude of the  $\zeta$  would reduce the homoaggregation within the water column and pore water  
11 of the substrate, which may reduce immobilization by pore space settling. Thus, retention was  
12 greater in the larger substrate (i.e., Cobble) for both NPs because there was more hyporheic  
13 exchange with subsequent physical and chemical immobilization within the substrate.  
14  
15  
16  
17  
18  
19  
20  
21  
22  
23  
24  
25  
26  
27  
28  
29  
30  
31  
32  
33  
34  
35  
36  
37  
38  
39  
40  
41  
42  
43  
44  
45  
46  
47  
48  
49  
50  
51  
52  
53  
54  
55  
56  
57  
58  
59  
60

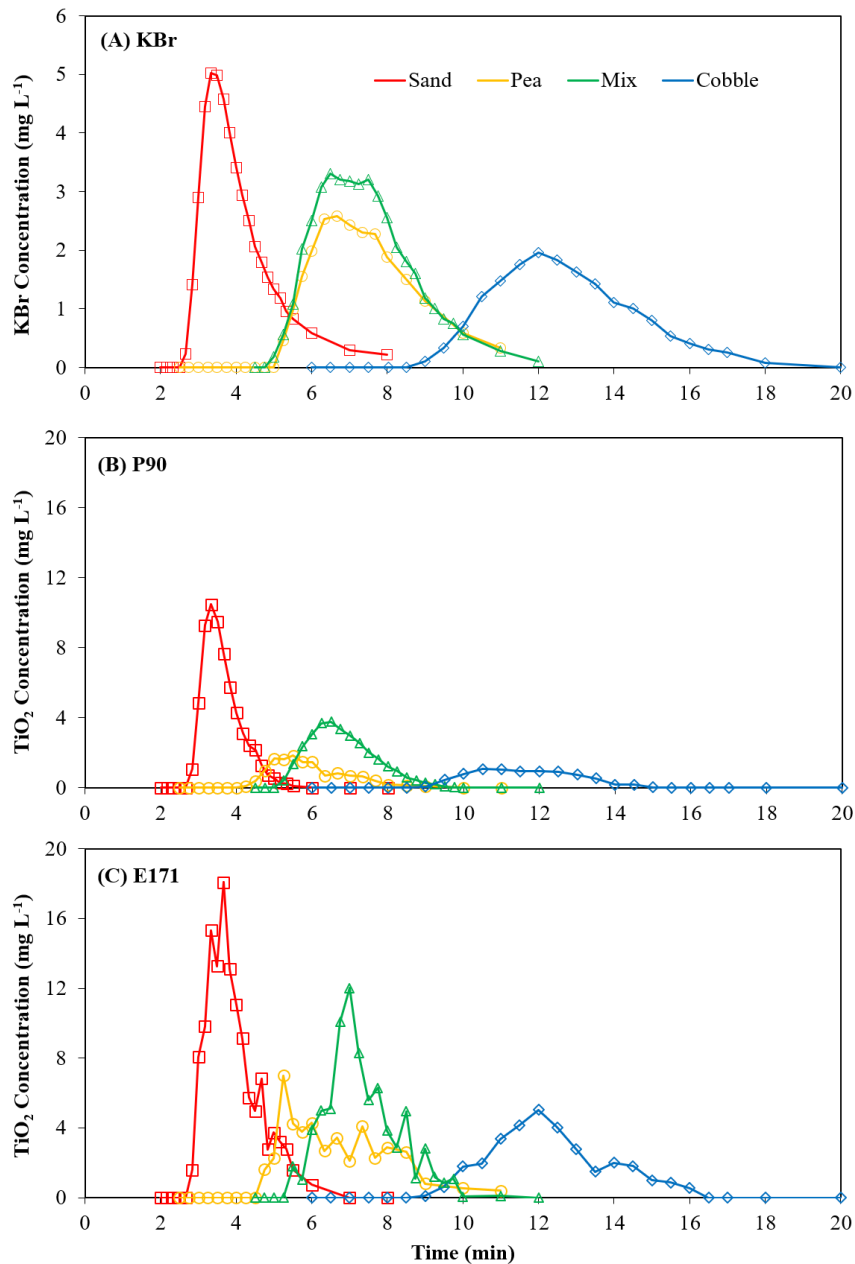


Figure 4. BTCs of pulse injections for (A) the conservative tracer (KBr), (B) P90, and (C) E171.

Experiments were conducted in June when biofilm growth in the stream was minimal. The BTCs represent samples taken at 40 m over a 20-min period.

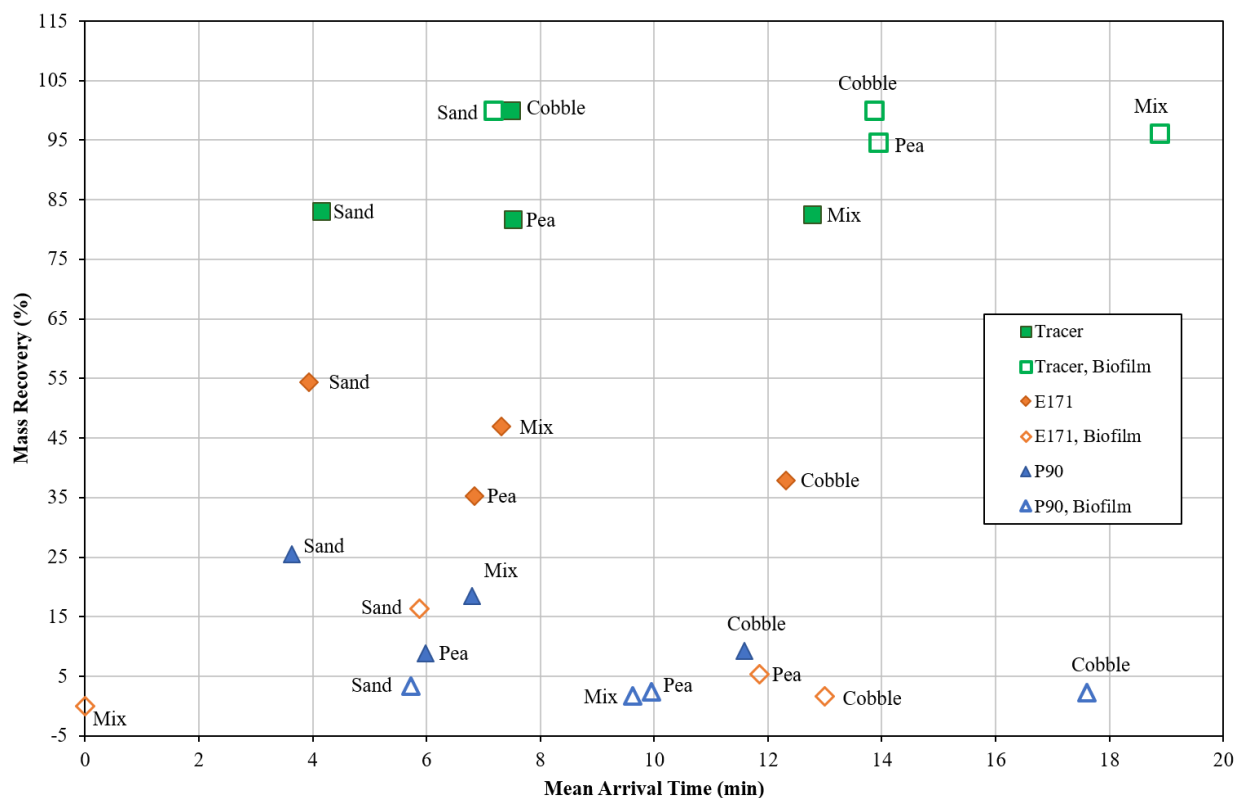


Figure 5. Mass recovery as a function of the mean arrival time for the conservative tracers, P90, and E171. All data was taken from the breakthrough curves for the 40 m sampling point (i.e., Figures 4 and 6). “Biofilm” indicates the September experiments when biofilms were flourishing.

### 3.3 Effect of Biofilm Growth on the Transport of P90 and E171

Pulse injection transport experiments were repeated in September after biofilms had flourished in the streams (i.e., Figure 2). Biofilm growth was spatially heterogeneous along the streams, with visually observed variations in surface growth, thickness, and formation within the pore structure of the streambed substrate and biomass in the water column. Figure 6 shows the BTCs for the tracer, P90, and E171 in the presence of enhanced biofilm growth, and the results of the moment analysis are provided in Table S2 with trends shown in Figure 5. The overall

1  
2  
3 transport behavior of the tracer and NPs was markedly different when biofilms were flourishing,  
4 with mean arrival times for nearly all conditions approximately 55-70% slower. The two notable  
5 exceptions were E171 in the Cobble and Mix streams, with approximately the same arrival time  
6 and no arrival observed, respectively. The increased plume spread for the NPs was likely due to  
7 the increased mixing caused by the presence of biofilm structures in the water column and  
8 streambed. The increased mean arrival times could have been caused by many factors, including  
9 longer flow pathways and enhanced regions of recirculation.

19 Under these biofilm conditions, the average mass recoveries for all streams for the tracer,  
20 P90, and E171 were  $100 \pm 5.4\%$ ,  $2.4 \pm 0.7\%$ , and  $5.8 \pm 7.3\%$ , respectively. The large difference  
21 in mass recovery between the conservative tracer and the NPs indicates that the presence of  
22 biofilms caused retention NPs, either through chemical or physical mechanisms. The mass  
23 recovery for NPs under flourishing biofilm conditions was significantly different compared to  
24 the mass recovery of the NPs under low biofilm conditions (P90,  $P = 0.041$ ; E171,  $P = 0.0017$ ).  
25 In fact, after experiments were completed, a visual inspection of the stream revealed obvious  
26 white sections of the biofilms where large amounts of the NPs had become trapped. Previous  
27 studies have also observed transfer of NPs to biofilms in various environmental settings.<sup>51, 87</sup>

40 Additionally, the mass recovery difference between the two NPs became insignificant ( $P$   
41  $= 0.38$ ) when biofilms were present. Though the mass recovery for E171 was as high as 16.3% in  
42 at 40 m in the Sand stream, no mass recovery was observed for the Mix stream. This dichotomy  
43 is presumably from the natural heterogeneous growth of biofilms in the streams, where large  
44 chunks of biofilm can attach to the side of the streams and remain in the water column (i.e.  
45 Figure 2), which would allow retention of suspended NPs. This is supported by comparing mass  
46 recoveries between the 20 m and 40 m sampling point for E171 in the Sand stream. When

1  
2  
3 biofilm growth was low, the mass recovery of E171 at the 20 and 40 m points was 60% and  
4  
5 54%, respectively. In comparison, when biofilms were flourishing, the mass recovery of E171 at  
6  
7 the 20 and 40 m points was 44% and 16%, respectively. The decrease in mass recovery as E171  
8  
9 was transported downstream was more drastic under flourishing biofilm conditions, presumably  
10  
11 due to the aforementioned heterogeneity. Similar results were observed for the Pea stream (Table  
12  
13 S2).  
14  
15  
16  
17  
18  
19  
20  
21  
22  
23  
24  
25  
26  
27  
28  
29  
30  
31  
32  
33  
34  
35  
36  
37  
38  
39  
40  
41  
42  
43  
44  
45  
46  
47  
48  
49  
50  
51  
52  
53  
54  
55  
56  
57  
58  
59  
60

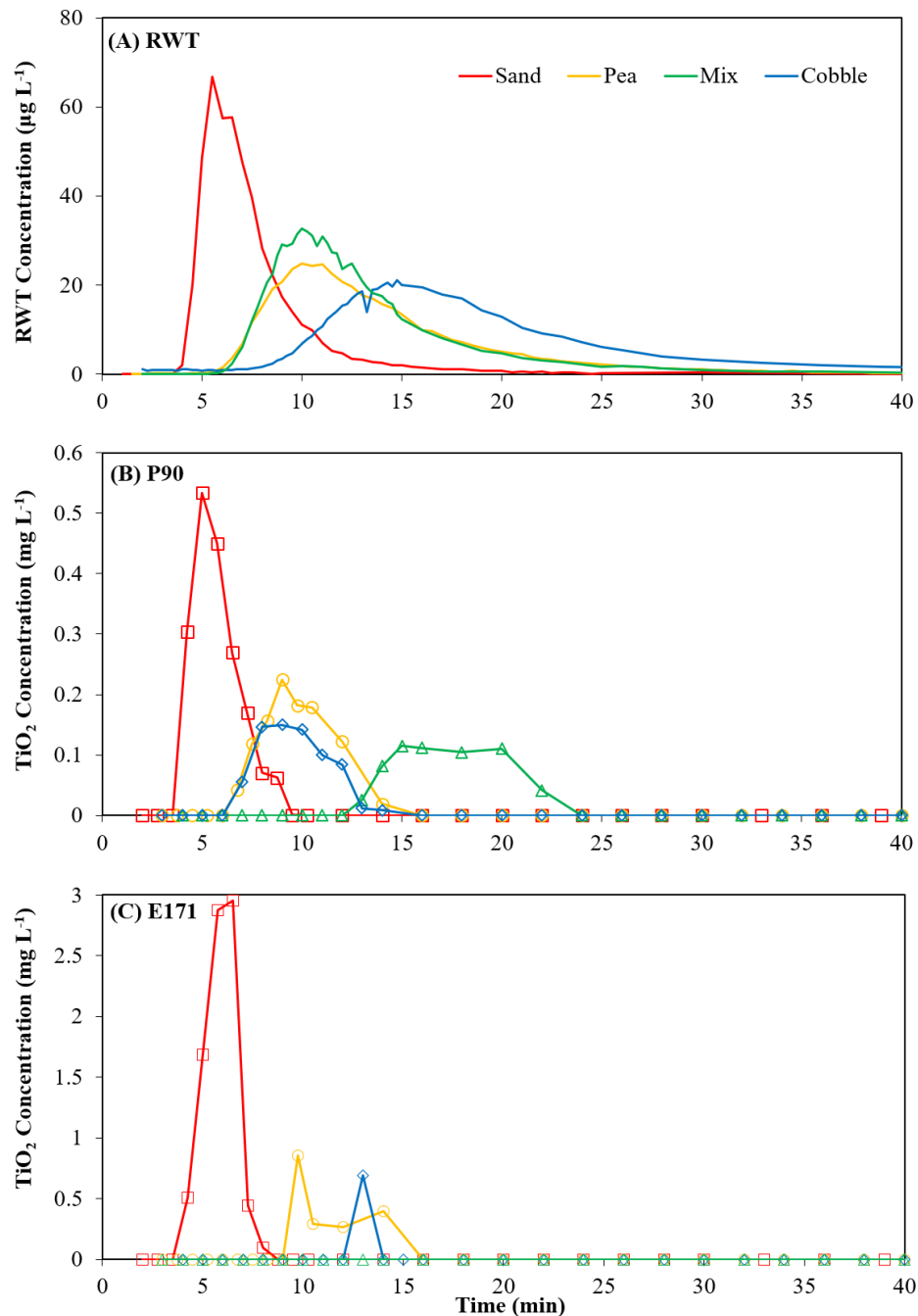


Figure 6. BTCs of pulse injections for (A) the conservative tracer, (B) P90, and (C) E171.

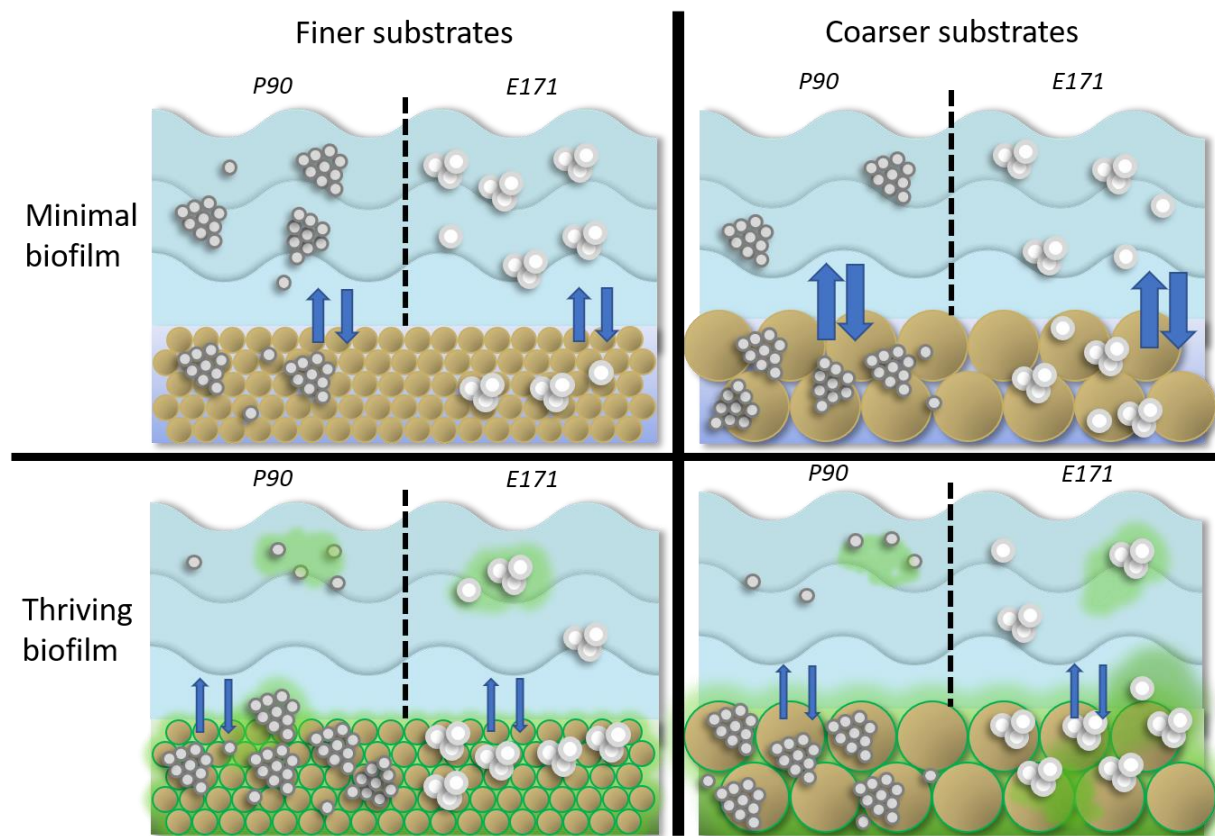
Experiments were conducted in June when biofilms were thriving. The BTCs represent samples taken at 40 m over a 40 m period. Sampling for the tracer was continuous (every 2 sec).

#### 4. CONCLUSIONS

The results presented herein highlight the importance of hyporheic exchange and biofilm growth in controlling the transport of NPs in streams, and conceptual schematic of these processes is shown in Figure 7. In streams where biofilm growth is minimal, transport of NPs will be controlled by mixing and hyporheic exchange and subsequent retention in the streambed substrate. When biofilms are flourishing, these will dominant immobilization of the NPs. The physico-chemical properties, especially the surface charge, of the NPs will affect aggregation and retention of NPs in the substrate, but this becomes less important in the presence of biofilms. Thus, in real streams, linking physico-chemical properties of pristine NPs to transport behavior may not be appropriate, as suggested previously.<sup>88</sup> Future studies should move toward creating sophisticated models that can capture the inherent variability of the streams by coupling datasets from controlled field streams with lab-scale substrate transport experiments.

While this study is one of the first to our knowledge to present estimates of the transport of TiO<sub>2</sub> NPs in field-scale streams with differing streambed substrate and biofilm conditions, there are limitations that exist due to experimental constraints. Foremost, experiments represented only a “pulse injection” scenario of a highly concentrated NP solution under relatively steady flow conditions. Likely, differing transport behavior will be observed with a continuous release of NPs to the streams, as observed previously for CeO<sub>2</sub> NPs.<sup>43</sup> With a continuous release, the concentration of NPs will be lower and that may reduce aggregation and settling tendencies allowing for increased mobility. Nonetheless, downstream transport of NPs will likely be limited, and thus accumulation within the geological and biological media is to be expected near discharge points (e.g., wastewater treatment plant effluents). This chronic accumulation may cause localized negative effects on the streambed habitats,<sup>89</sup> with unintended

1  
2  
3 negative consequences for stream ecological structure and function.<sup>90</sup> Additionally, storm events  
4 and higher flows are expected to cause resuspension of the NPs from the streambed substrate,<sup>42</sup>  
5 potentially moving them further downstream. The stream water used had relatively high ionic  
6 strength that was low in TSS and DOC. NP homoaggregation would be reduced in lower ionic  
7 strength waters, while higher TSS and DOC could enhance heteroaggregation and mobility,  
8 respectively. To enhance our understanding of NP transport in stream networks, further studies  
9 are needed with increased complexity at the field-scale involving geological collectors (e.g., clay  
10 particles), DOC, and organisms.  
11  
12  
13  
14  
15  
16  
17  
18  
19  
20  
21  
22  
23



24  
25  
26  
27  
28  
29  
30  
31  
32  
33  
34  
35  
36  
37  
38  
39  
40  
41  
42  
43  
44  
45  
46  
47  
48  
49  
50  
51  
52 Figure 7. Conceptualization of processes affecting NP transport in streams under the experiment  
53 conditions tested. Both NPs undergo homoaggregation in the streams, which is more severe for  
54  
55  
56  
57  
58  
59  
60

1  
2  
3 P90. Hyporheic exchange is greater for coarser substrates (indicated by the thickness of the  
4 vertical blue arrows). This allows for increased interaction between the NPs and the substrate  
5 resulting in increased retention. Biofilms can grow suspended in the water column, on the  
6 benthic layer, or within the pore spaces of the substrate. When biofilms are flourishing,  
7 hyporheic exchange is reduced, but they increase the retention of NPs and it is similar for P90  
8 and E171 and across streams.  
9  
10  
11  
12  
13  
14  
15  
16  
17  
18  
19  
20  
21  
22  
23  
24  
25  
26  
27  
28  
29  
30  
31  
32  
33  
34  
35  
36  
37  
38  
39  
40  
41  
42  
43  
44  
45  
46  
47  
48  
49  
50  
51  
52  
53  
54  
55  
56  
57  
58  
59  
60

## ACKNOWLEDGEMENTS

This material is based upon work supported by the National Science Foundation under grant no. CBET-1705770. Additional support for Mr. Junyeol Kim came from the CEST/Bayer Predoctoral Research Fellowship [Center for Environmental Science and Technology at Notre Dame (CEST)]. We especially want to thank the Notre Dame Environmental Change Initiation (ECI) for seed grant funding and ND-LEEF for use of the experimental streams. The authors thank CEST for access to instrumentation, including the IC, ICP-OES, and microwave digester. Lastly, we would like to thank Prof. Jennifer Tank and Mr. Brett Peters for their help setting up experiments at ND-LEEF.

## REFERENCES

1. Q. Zhang, J.-Q. Huang, W.-Z. Qian, Y.-Y. Zhang and F. Wei, The Road for Nanomaterials Industry: A Review of Carbon Nanotube Production, Post-Treatment, and Bulk Applications for Composites and Energy Storage, *Small*, 2013, **9**, 1237-1265.
2. B. Pan and B. Xing, Applications and implications of manufactured nanoparticles in soils: a review, *European Journal of Soil Science*, 2012, **63**, 437-456.
3. M. F. L. De Volder, S. H. Tawfick, R. H. Baughman and A. J. Hart, Carbon Nanotubes: Present and Future Commercial Applications, *Science*, 2013, **339**, 535.
4. Z. Fei Yin, L. Wu, H. Gui Yang and Y. Hua Su, Recent progress in biomedical applications of titanium dioxide, *Physical Chemistry Chemical Physics*, 2013, **15**, 4844-4858.
5. A. A. Keller, W. Vosti, H. Wang and A. Lazareva, Release of engineered nanomaterials from personal care products throughout their life cycle, *Journal of Nanoparticle Research*, 2014, **16**, 2489.
6. A. A. Keller, S. McFerran, A. Lazareva and S. Suh, Global life cycle releases of engineered nanomaterials, *Journal of Nanoparticle Research*, 2013, **15**, 1692.
7. R. F. Domingos, N. Tufenkji and K. J. Wilkinson, Aggregation of Titanium Dioxide Nanoparticles: Role of a Fulvic Acid, *Environmental Science & Technology*, 2009, **43**, 1282-1286.
8. E. M. Hotze, T. Phenrat and G. V. Lowry, Nanoparticle Aggregation: Challenges to Understanding Transport and Reactivity in the Environment, *Journal of Environmental Quality*, 2010, **39**, 1909-1924.
9. D. H. Lin, X. L. Tian, F. C. Wu and B. S. Xing, Fate and Transport of Engineered Nanomaterials in the Environment, *Journal of Environmental Quality*, 2010, **39**, 1896-1908.
10. A. R. Petosa, D. P. Jaisi, I. R. Quevedo, M. Elimelech and N. Tufenkji, Aggregation and Deposition of Engineered Nanomaterials in Aquatic Environments: Role of Physicochemical Interactions, *Environmental Science & Technology*, 2010, **44**, 6532-6549.
11. Y. G. Wang, Y. S. Li, H. Kim, S. L. Walker, L. M. Abriola and K. D. Pennell, Transport and Retention of Fullerene Nanoparticles in Natural Soils, *Journal of Environmental Quality*, 2010, **39**, 1925-1933.
12. T. Phenrat, J. E. Song, C. M. Cisneros, D. P. Schoenfelder, R. D. Tilton and G. V. Lowry, Estimating Attachment of Nano- and Submicrometer-particles Coated with Organic Macromolecules in Porous Media: Development of an Empirical Model, *Environmental Science & Technology*, 2010, **44**, 4531-4538.
13. S. Torkzaban, Y. Kim, M. Mulvihill, J. M. Wan and T. K. Tokunaga, Transport and deposition of functionalized CdTe nanoparticles in saturated porous media, *Journal of Contaminant Hydrology*, 2010, **118**, 208-217.
14. K. D. Hristovski, P. K. Westerhoff and J. D. Posner, Octanol-water distribution of engineered nanomaterials, *Journal of Environmental Science and Health Part a-Toxic/Hazardous Substances & Environmental Engineering*, 2011, **46**, 636-647.
15. A. R. Petosa, S. J. Brennan, F. Rajput and N. Tufenkji, Transport of two metal oxide nanoparticles in saturated granular porous media: Role of water chemistry and particle coating, *Water Research*, 2012, **46**, 1273-1285.
16. D. X. Zhou, A. I. Abdel-Fattah and A. A. Keller, Clay Particles Destabilize Engineered Nanoparticles in Aqueous Environments, *Environmental Science & Technology*, 2012, **46**, 7520-7526.
17. J. A. Nason, S. A. McDowell and T. W. Callahan, Effects of natural organic matter type and concentration on the aggregation of citrate-stabilized gold nanoparticles, *Journal of Environmental Monitoring*, 2012, **14**, 1885-1892.

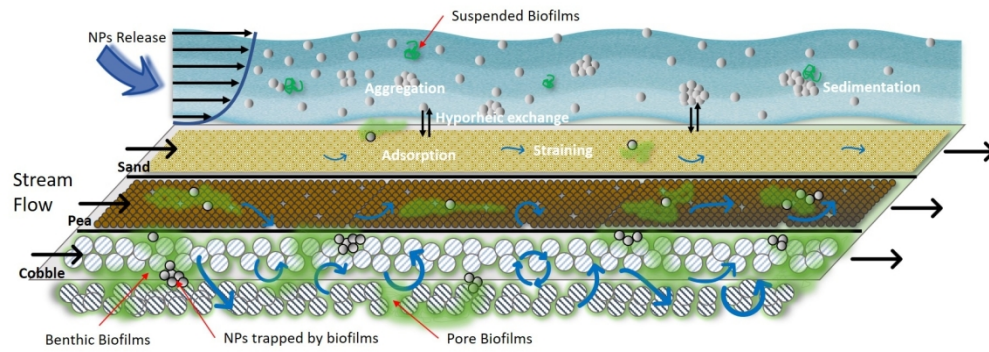
18. Y. Xiao and M. R. Wiesner, Transport and Retention of Selected Engineered Nanoparticles by Porous Media in the Presence of a Biofilm, *Environmental Science & Technology*, 2013, **47**, 2246-2253.
19. J. Yang, J. L. Bitter, B. A. Smith, D. H. Fairbrother and W. P. Ball, Transport of Oxidized Multi-Walled Carbon Nanotubes through Silica Based Porous Media: Influences of Aquatic Chemistry, Surface Chemistry, and Natural Organic Matter, *Environmental Science & Technology*, 2013, **47**, 14034-14043.
20. M. T. Zhu, G. J. Nie, H. Meng, T. Xia, A. Nel and Y. L. Zhao, Physicochemical Properties Determine Nanomaterial Cellular Uptake, Transport, and Fate, *Accounts of Chemical Research*, 2013, **46**, 622-631.
21. Z. C. Qi, L. Hou, D. Q. Zhu, R. Ji and W. Chen, Enhanced Transport of Phenanthrene and 1-Naphthol by Colloidal Graphene Oxide Nanoparticles in Saturated Soil, *Environmental Science & Technology*, 2014, **48**, 10136-10144.
22. M. Zhu, H. T. Wang, A. A. Keller, T. Wang and F. T. Li, The effect of humic acid on the aggregation of titanium dioxide nanoparticles under different pH and ionic strengths, *Science of the Total Environment*, 2014, **487**, 375-380.
23. A. Praetorius, N. Tufenkji, K. U. Goss, M. Scheringer, F. von der Kammer and M. Elimelech, The road to nowhere: equilibrium partition coefficients for nanoparticles, *Environ.-Sci. Nano*, 2014, **1**, 317-323.
24. E. Goldberg, M. Scheringer, T. D. Bucheli and K. Hungerbuehler, Prediction of nanoparticle transport behavior from physicochemical properties: machine learning provides insights to guide the next generation of transport models, *Environ.-Sci. Nano*, 2015, **2**, 352-360.
25. A. L. Dale, G. V. Lowry and E. A. Casman, Much ado about alpha: reframing the debate over appropriate fate descriptors in nanoparticle environmental risk modeling, *Environ.-Sci. Nano*, 2015, **2**, 27-32.
26. I. L. Molnar, W. P. Johnson, J. I. Gerhard, C. S. Willson and D. M. O'Carroll, Predicting colloid transport through saturated porous media: A critical review, *Water Resour. Res.*, 2015, **51**, 6804-6845.
27. Y. Y. Sun, B. Gao, S. A. Bradford, L. Wu, H. Chen, X. Q. Shi and J. C. Wu, Transport, retention, and size perturbation of graphene oxide in saturated porous media: Effects of input concentration and grain size, *Water Research*, 2015, **68**, 24-33.
28. D. L. Karwan and J. E. Saiers, Hyporheic exchange and streambed filtration of suspended particles, *Water Resources Research*, 2012, **48**, 12.
29. F. Boano, J. W. Harvey, A. Marion, A. I. Packman, R. Revelli, L. Ridolfi and A. Worman, Hyporheic flow and transport processes: Mechanisms, models, and biogeochemical implications, *Reviews of Geophysics*, 2014, **52**, 603-679.
30. B. P. Espinasse, N. K. Geitner, A. Schierz, M. Therezien, C. J. Richardson, G. V. Lowry, L. Ferguson and M. R. Wiesner, Comparative Persistence of Engineered Nanoparticles in a Complex Aquatic Ecosystem, *Environmental Science & Technology*, 2018, **52**, 4072-4078.
31. N. K. Geitner, N. J. O'Brien, A. A. Turner, E. J. Cummins and M. R. Wiesner, Measuring Nanoparticle Attachment Efficiency in Complex Systems, *Environmental Science & Technology*, 2017, **51**, 13288-13294.
32. A. A. Markus, J. R. Parsons, E. W. M. Roex, P. de Voogt and R. Laane, Modelling the transport of engineered metallic nanoparticles in the river Rhine, *Water Research*, 2016, **91**, 214-224.
33. L. E. Barton, M. Auffan, L. Olivi, J. Y. Bottero and M. R. Wiesner, Heteroaggregation, transformation and fate of CeO<sub>2</sub> nanoparticles in wastewater treatment, *Environmental Pollution*, 2015, **203**, 122-129.

- 1  
2  
3  
4  
5  
6  
7  
8  
9  
10  
11  
12  
13  
14  
15  
16  
17  
18  
19  
20  
21  
22  
23  
24  
25  
26  
27  
28  
29  
30  
31  
32  
33  
34  
35  
36  
37  
38  
39  
40  
41  
42  
43  
44  
45  
46  
47  
48  
49  
50  
51  
52  
53  
54  
55  
56  
57  
58  
59  
60
34. J. Labille, C. Harns, J. Y. Bottero and J. Brant, Heteroaggregation of Titanium Dioxide Nanoparticles with Natural Clay Colloids, *Environmental Science & Technology*, 2015, **49**, 6608-6616.
  35. J. B. Liu, Y. S. Hwang and J. J. Lenhart, Heteroaggregation of bare silver nanoparticles with clay minerals, *Environmental Science-Nano*, 2015, **2**, 528-540.
  36. A. A. Markus, J. R. Parsons, E. W. M. Roex, P. de Voogt and R. Laane, Modeling aggregation and sedimentation of nanoparticles in the aquatic environment, *Science of the Total Environment*, 2015, **506**, 323-329.
  37. A. Praetorius, J. Labille, M. Scheringer, A. Thill, K. Hungerbuhler and J. Y. Bottero, Heteroaggregation of Titanium Dioxide Nanoparticles with Model Natural Colloids under Environmentally Relevant Conditions, *Environmental Science & Technology*, 2014, **48**, 10690-10698.
  38. J. T. K. Quik, I. Velzeboer, M. Wouterse, A. A. Koelmans and D. van de Meent, Heteroaggregation and sedimentation rates for nanomaterials in natural waters, *Water Research*, 2014, **48**, 269-279.
  39. I. Velzeboer, J. T. K. Quik, D. van de Meent and A. A. Koelmans, RAPID SETTLING OF NANOPARTICLES DUE TO HETEROAGGREGATION WITH SUSPENDED SEDIMENT, *Environmental Toxicology and Chemistry*, 2014, **33**, 1766-1773.
  40. J. T. K. Quik, M. C. Stuart, M. Wouterse, W. Peijnenburg, A. J. Hendriks and D. van de Meent, Natural colloids are the dominant factor in the sedimentation of nanoparticles, *Environmental Toxicology and Chemistry*, 2012, **31**, 1019-1022.
  41. T. Areepitak and J. H. Ren, Model Simulations of Particle Aggregation Effect on Colloid Exchange between Streams and Streambeds, *Environmental Science & Technology*, 2011, **45**, 5614-5621.
  42. N. T. Boncagni, J. M. Otaegui, E. Warner, T. Curran, J. H. Ren and M. M. F. De Cortalezzi, Exchange of TiO<sub>2</sub> Nanoparticles between Streams and Streambeds, *Environmental Science & Technology*, 2009, **43**, 7699-7705.
  43. L. F. Baker, R. S. King, J. M. Unrine, B. T. Castellon, G. V. Lowry and C. W. Matson, PRESS OR PULSE EXPOSURES DETERMINE THE ENVIRONMENTAL FATE OF CERIUM NANOPARTICLES IN STREAM MESOCOSMS, *Environmental Toxicology and Chemistry*, 2016, **35**, 1213-1223.
  44. N. K. Geitner, J. L. Cooper, A. Avellan, B. T. Castellon, B. G. Perrotta, N. Bossa, M. Simonin, S. M. Anderson, S. Inoue, M. F. Hochella, C. J. Richardson, E. S. Bernhardt, G. V. Lowry, P. L. Ferguson, C. W. Matson, R. S. King, J. M. Unrine, M. R. Wiesner and H. Hsu-Kim, Size-Based Differential Transport, Uptake, and Mass Distribution of Ceria (CeO<sub>2</sub>) Nanoparticles in Wetland Mesocosms, *Environmental Science & Technology*, 2018, **52**, 9768-9776.
  45. K. L. Garner and A. A. Keller, Emerging patterns for engineered nanomaterials in the environment: a review of fate and toxicity studies, *Journal of Nanoparticle Research*, 2014, **16**, 28.
  46. N. Solovitch, J. Labille, J. Rose, P. Chaurand, D. Borschneck, M. R. Wiesner and J. Y. Bottero, Concurrent Aggregation and Deposition of TiO<sub>2</sub> Nanoparticles in a Sandy Porous Media, *Environmental Science & Technology*, 2010, **44**, 4897-4902.
  47. S. Arnon, L. P. Marx, K. E. Searcy and A. I. Packman, Effects of overlying velocity, particle size, and biofilm growth on stream--subsurface exchange of particles, *Hydrological Processes*, 2010, **24**, 108-114.
  48. J. Fabrega, R. Zhang, J. C. Renshaw, W. T. Liu and J. R. Lead, Impact of silver nanoparticles on natural marine biofilm bacteria, *Chemosphere*, 2011, **85**, 961-966.
  49. J. Z. He, C. C. Li, D. J. Wang and D. M. Zhou, Biofilms and extracellular polymeric substances mediate the transport of graphene oxide nanoparticles in saturated porous media, *Journal of Hazardous Materials*, 2015, **300**, 467-474.

- 1  
2  
3  
4 50. X. J. Jiang, X. T. Wang, M. P. Tong and H. Kim, Initial transport and retention behaviors of ZnO  
5 nanoparticles in quartz sand porous media coated with Escherichia coli biofilm, *Environmental*  
6 *Pollution*, 2013, **174**, 38-49.
- 7 51. K. J. Kulacki, B. J. Cardinale, A. A. Keller, R. Bier and H. Dickson, How do stream organisms  
8 respond to, and influence, the concentration of titanium dioxide nanoparticles? A mesocosm  
9 study with algae and herbivores, *Environmental Toxicology and Chemistry*, 2012, **31**, 2414-2422.
- 10 52. R. N. Lerner, Q. Lu, H. Zeng and Y. Liu, The effects of biofilm on the transport of stabilized  
11 zerovalent iron nanoparticles in saturated porous media, *Water Research*, 2012, **46**, 975-985.
- 12 53. M. Crampon, J. Hellal, C. Mouvet, G. Wille, C. Michel, A. Wiener, J. Braun and P. Ollivier, Do  
13 natural biofilm impact nZVI mobility and interactions with porous media? A column study,  
14 *Science of the Total Environment*, 2018, **610**, 709-719.
- 15 54. M. V. Wright, C. W. Matson, L. F. Baker, B. T. Castellon, P. S. Watkins and R. S. King, Titanium  
16 dioxide nanoparticle exposure reduces algal biomass and alters algal assemblage composition in  
17 wastewater effluent-dominated stream mesocosms, *Science of the Total Environment*, 2018,  
18 **626**, 357-365.
- 19 55. T. J. Battin, F. V. D. Kammer, A. Weilhartner, S. Ottofuelling and T. Hofmann, Nanostructured  
20 TiO<sub>2</sub>: Transport Behavior and Effects on Aquatic Microbial Communities under Environmental  
21 Conditions, *Environmental Science & Technology*, 2009, **43**, 8098-8104.
- 22 56. C. T. T. Binh, E. Adams, E. Vigen, T. Z. Tong, M. A. Alsina, J. F. Gaillard, K. A. Gray, C. G. Peterson  
23 and J. J. Kelly, Chronic addition of a common engineered nanomaterial alters biomass, activity  
24 and composition of stream biofilm communities, *Environmental Science-Nano*, 2016, **3**, 619-630.
- 25 57. M. Button, H. Auvinen, F. Van Koetsem, B. Hosseinkhani, D. Rousseau, K. P. Weber and G. Du  
26 Laing, Susceptibility of constructed wetland microbial communities to silver nanoparticles: A  
27 microcosm study, *Ecological Engineering*, 2016, **97**, 476-485.
- 28 58. M. A. Maurer-Jones, I. L. Gunsolus, B. M. Meyer, C. J. Christenson and C. L. Haynes, Impact of  
29 TiO<sub>2</sub> nanoparticles on growth, biofilm formation, and flavin secretion in *Shewanella oneidensis*,  
30 *Analytical chemistry*, 2013, **85**, 5810-5818.
- 31 59. A. Ozaki, E. Adams, C. Binh, T. Z. Tong, J. F. Gaillard, K. A. Gray and J. J. Kelly, One-Time Addition  
32 of Nano-TiO<sub>2</sub> Triggers Short-Term Responses in Benthic Bacterial Communities in Artificial  
33 Streams, *Microbial Ecology*, 2016, **71**, 266-275.
- 34 60. A. Weir, P. Westerhoff, L. Fabricius, K. Hristovski and N. von Goetz, Titanium Dioxide  
35 Nanoparticles in Food and Personal Care Products, *Environmental Science & Technology*, 2012,  
36 **46**, 2242-2250.
- 37 61. H. B. Shi, R. Magaye, V. Castranova and J. S. Zhao, Titanium dioxide nanoparticles: a review of  
38 current toxicological data, *Particle and Fibre Toxicology*, 2013, **10**, 33.
- 39 62. I. S. Sohal, K. S. O'Fallon, P. Gaines, P. Demokritou and D. Bello, Ingested engineered  
40 nanomaterials: state of science in nanotoxicity testing and future research needs, *Particle and*  
41 *Fibre Toxicology*, 2018, **15**, 31.
- 42 63. W. Dufou, H. Terrisse, M. Richard-Plouet, E. Gautron, F. Popa, B. Humbert and M. H. Ropers,  
43 Criteria to define a more relevant reference sample of titanium dioxide in the context of food: a  
44 multiscale approach, *Food Additives and Contaminants Part a-Chemistry Analysis Control*  
45 *Exposure & Risk Assessment*, 2017, **34**, 653-665.
- 46 64. J. J. Faust, K. Doudrick, Y. Yang, P. Westerhoff and D. G. Capco, Food grade titanium dioxide  
47 disrupts intestinal brush border microvilli in vitro independent of sedimentation, *Cell Biology*  
48 *and Toxicology*, 2014, **30**, 169-188.
- 49 65. Y. Yang, K. Doudrick, X. Y. Bi, K. Hristovski, P. Herckes, P. Westerhoff and R. Kaegi,  
50 Characterization of Food-Grade Titanium Dioxide: The Presence of Nanosized Particles,  
51 *Environmental Science & Technology*, 2014, **48**, 6391-6400.
- 52  
53  
54  
55  
56  
57  
58  
59  
60

- 1  
2  
3  
4  
5  
6  
7  
8  
9  
10  
11  
12  
13  
14  
15  
16  
17  
18  
19  
20  
21  
22  
23  
24  
25  
26  
27  
28  
29  
30  
31  
32  
33  
34  
35  
36  
37  
38  
39  
40  
41  
42  
43  
44  
45  
46  
47  
48  
49  
50  
51  
52  
53  
54  
55  
56  
57  
58  
59  
60
66. J. Kim and K. Doudrick, Emerging investigator series: protein adsorption and transformation on catalytic and food-grade TiO<sub>2</sub> nanoparticles in the presence of dissolved organic carbon, *Environmental Science-Nano*, 2019, **6**, 1688-1703.
67. R. Yusoff, M. H. Kathawala, L. T. H. Nguyen, M. I. Setyawati, P. Chiew, Y. S. Wu, A. L. Ch'ng, Z. M. Wang and K. W. Ng, Biomolecular interaction and kinematics differences between P25 and E171 TiO<sub>2</sub> nanoparticles, *Nanoimpact*, 2018, **12**, 51-57.
68. K. Doudrick, O. Monz<sup>{\o}</sup>n, A. Mangonon, K. Hristovski and P. Westerhoff, Nitrate Reduction in Water Using Commercial Titanium Dioxide Photocatalysts (P25, P90, and Hombikat {UV}100), *Journal of Environmental Engineering*, 2011, 423.
69. Y. Yang, K. Doudrick, X. Bi, K. Hristovski, P. Herckes, P. Westerhoff and R. Kaegi, Characterization of Food-Grade Titanium Dioxide: The Presence of Nanosized Particles, *Environmental Science & Technology*, 2014, **48**, 6391-6400.
70. J. Kim and K. Doudrick, Emerging investigator series: protein adsorption and transformation on catalytic and food-grade TiO<sub>2</sub> nanoparticles in the presence of dissolved organic carbon, *Environmental Science: Nano*, 2019.
71. A. J. Shogren, J. L. Tank, E. Andruszkiewicz, B. Olds, A. R. Mahon, C. L. Jerde and D. Bolster, Controls on eDNA movement in streams: Transport, Retention, and Resuspension, *Scientific Reports*, 2017, **7**, 11.
72. A. F. Aubeneau, B. Hanrahan, D. Bolster and J. Tank, Biofilm growth in gravel bed streams controls solute residence time distributions, *Journal of Geophysical Research: Biogeosciences*, 2016, **121**, 1840-1850.
73. A. F. Aubeneau, B. Hanrahan, D. Bolster and J. L. Tank, Substrate size and heterogeneity control anomalous transport in small streams, *Geophysical Research Letters*, 2014, **41**, 8335-8341.
74. C. L. Jerde, B. P. Olds, A. J. Shogren, E. A. Andruszkiewicz, A. R. Mahon, D. Bolster and J. L. Tank, Influence of Stream Bottom Substrate on Retention and Transport of Vertebrate Environmental DNA, *Environmental Science & Technology*, 2016, **50**, 8770-8779.
75. K. R. Roche, A. J. Shogren, A. Aubeneau, J. L. Tank and D. Bolster, Modeling Benthic Versus Hyporheic Nutrient Uptake in Unshaded Streams With Varying Substrates, *Journal of Geophysical Research-Biogeosciences*, 2019, **124**, 367-383.
76. B. R. Hanrahan, J. L. Tank, A. J. Shogren and E. J. Rosi, Using the raz-rru method to examine linkages between substrate, biofilm colonisation and stream metabolism in open-canopy streams, *Freshwater Biology*, 2018, **63**, 1610-1624.
77. R. J. O. Hall and J. L. Tank, Ecosystem metabolism controls nitrogen uptake in streams in Grand Teton National Park, Wyoming, *Limnology and Oceanography*, 2003, **48**, 1120-1128.
78. P. C. Leube, W. Nowak and G. Schneider, Temporal moments revisited: Why there is no better way for physically based model reduction in time, *Water Resources Research*, 2012, **48**.
79. A. J. Valocchi, Use of temporal moment analysis to study reactive solute transport in aggregated porous media, *Geoderma*, 1990, **46**, 233-247.
80. V. Renu and G. S. Kumar, Temporal moment analysis of solute transport in a coupled fracture-skin-matrix system, *Sadhana*, 2014, **39**, 487-509.
81. M. B. Romanello and M. M. F. de Cortalezzi, An experimental study on the aggregation of TiO<sub>2</sub> nanoparticles under environmentally relevant conditions, *Water Research*, 2013, **47**, 3887-3898.
82. R. A. French, A. R. Jacobson, B. Kim, S. L. Isley, R. L. Penn and P. C. Baveye, Influence of Ionic Strength, pH, and Cation Valence on Aggregation Kinetics of Titanium Dioxide Nanoparticles, *Environmental Science & Technology*, 2009, **43**, 1354-1359.
83. X. Y. Liu, G. X. Chen and C. M. Su, Effects of material properties on sedimentation and aggregation of titanium dioxide nanoparticles of anatase and rutile in the aqueous phase, *Journal of Colloid and Interface Science*, 2011, **363**, 84-91.

- 1  
2  
3 84. P. Guo, N. Xu, D. Li, X. X. Huangfu and Z. L. Li, Aggregation and transport of rutile titanium  
4 dioxide nanoparticles with montmorillonite and diatomite in the presence of phosphate in  
5 porous sand, *Chemosphere*, 2018, **204**, 327-334.  
6  
7 85. D. L. Karwan and J. E. Saiers, Hyporheic exchange and streambed filtration of suspended  
8 particles, *Water Resour. Res.*, 2012, **48**.  
9  
10 86. W. Zhang, J. Crittenden, K. G. Li and Y. S. Chen, Attachment Efficiency of Nanoparticle  
11 Aggregation in Aqueous Dispersions: Modeling and Experimental Validation, *Environmental  
12 Science & Technology*, 2012, **46**, 7054-7062.  
13  
14 87. J. L. Ferry, P. Craig, C. Hexel, P. Sisco, R. Frey, P. L. Pennington, M. H. Fulton, I. G. Scott, A. W.  
15 Decho, S. Kashiwada, C. J. Murphy and T. J. Shaw, Transfer of gold nanoparticles from the water  
16 column to the estuarine food web, *Nature Nanotechnology*, 2009, **4**, 441-444.  
17  
18 88. M. C. Surette, J. A. Nason and R. Kaegi, The influence of surface coating functionality on the  
19 aging of nanoparticles in wastewater, *Environmental Science: Nano*, 2019.  
20  
21 89. A. J. Boulton, Hyporheic rehabilitation in rivers: restoring vertical connectivity, *Freshwater  
22 Biology*, 2007, **52**, 632-650.  
23  
24  
25  
26  
27  
28  
29  
30  
31  
32  
33  
34  
35  
36  
37  
38  
39  
40  
41  
42  
43  
44  
45  
46  
47  
48  
49  
50  
51  
52  
53  
54  
55  
56  
57  
58  
59  
60



306x113mm (150 x 150 DPI)

1  
2  
3  
4  
5  
6  
7  
8  
9  
10  
11  
12  
13  
14  
15  
16  
17  
18  
19  
20  
21  
22  
23  
24  
25  
26  
27  
28  
29  
30  
31  
32  
33  
34  
35  
36  
37  
38  
39  
40  
41  
42  
43  
44  
45  
46  
47  
48  
49  
50  
51  
52  
53  
54  
55  
56  
57  
58  
59  
60